

Optical Conductivity in Mott-Hubbard Systems

M. J. Rozenberg*, G. Kotliar, and H. Kajueter

Serin Physics Laboratory, Rutgers University, Piscataway, NJ 08855-0849

G. A. Thomas and D. H. Rapkine

AT&T Bell Laboratories, Murray Hill, NJ 07974-0636

J. M. Honig and P. Metcalf

Department of Chemistry, Purdue University, West Lafayette, IN 47907

Abstract

We study the transfer of spectral weight in the optical spectra of a strongly correlated electron system as a function of temperature and interaction strength. Within a dynamical mean field theory of the Hubbard model that becomes exact in the limit of large lattice coordination, we predict an anomalous enhancement of spectral weight as a function of temperature in the correlated metallic state and report on experimental measurements which agree with this prediction in V_2O_3 . We argue that the optical conductivity anomalies in the metal are connected to the proximity to a crossover region in the phase diagram of the model.

71.27.+a, 71.30.+h, 78

The interest in the distribution of spectral weight in the optical conductivity of correlated electron systems has been revived by the improvement in the quality of the experimental data [1,2]. The traditional theoretical methods used in the strong correlation problem, have only been partially successful in describing the interesting behavior of the optical response which takes place in the strong correlation regime. This is most notable when the temperature dependence of the spectral weight is considered. We present here new optical conductivity data on metallic V_2O_3 and analyze the problem theoretically it using a mean field theory which is exact in the limit of large number of spatial dimensions [3]. In this limit, lattice models can be mapped onto an equivalent impurity model subject to a selfconsistency condition for the conduction electron bath [4,5]. This technique has already given some new insights into the Mott transition, which is realized in the solution of the Hubbard model [6–9]. The new experimental measurements on V_2O_3 test a critical prediction of the theory.

The goal of this paper is to demonstrate two points: *i)* that the present dynamical mean field approach is *a useful tool* which allows us to make qualitative predictions such as an anomalous enhancement of spectral weight as a function of temperature. This behavior of the spectral weight is confirmed by experiments in V_2O_3 reported here; and *ii)* that the Hubbard model on a *frustrated* lattice, in the limit of large lattice coordination, with parameters extracted from the optical data, accounts for many other experimental features of the V_2O_3 system, such as its phase diagram and large specific heat capacity. We also present results for the various quantities which are useful in the analysis of the optical conductivity of the Hubbard model, treated in an approximation which is exact in a well defined limit.

The experiments were carried out on single crystals of V_2O_3 which were grown by the skull-melting process, carefully annealed, polished and mounted on a temperature-controlled stage in an optical cryostat [1,10]. The specular reflectivity was measured using a Fourier transform spectrometer over a frequency range from $6meV$ to $3.7eV$. The data were combined with dc conductivity and higher energy reflectivity measurements, and a Kramers-Kronig transformation was used to determine the conductivity.

The theoretical model is the Hubbard hamiltonian,

$$H = - \sum_{\langle i,j \rangle} (t_{ij} + \mu) c_{i\sigma}^\dagger c_{j\sigma} + \sum_i U (n_{i\uparrow} - \frac{1}{2})(n_{i\downarrow} - \frac{1}{2}) \quad (1)$$

where summation over repeated spin indices is assumed.

In the limit of infinite dimensions the coordination number of the lattice (i.e. the number of neighbors q) gets large and the hopping is scaled as $t_{ij} \rightarrow \frac{t}{\sqrt{q}}$ [3]. The lattice model is mapped onto an equivalent impurity problem supplemented by a selfconsistency condition. The derivation of this result can be found elsewhere [4,5], so we only present the final expressions. The resulting local effective action reads,

$$S_{local} = - \int_0^\beta d\tau \int_0^\beta d\tau' c_\sigma^\dagger(\tau) G_0^{-1}(\tau - \tau') c_\sigma(\tau') + U \int_0^\beta d\tau (n_\uparrow(\tau) - \frac{1}{2})(n_\downarrow(\tau) - \frac{1}{2}) \quad (2)$$

where c_σ^\dagger , c_σ correspond to a particular site. Requiring that $G_{local}(\omega) = \Sigma_k G(k, \omega)$ the selfconsistency condition becomes $G_0^{-1}(\omega) = \omega + \mu - t^2 G_{local}(\omega)$, where we have assumed a semi-circular bare density of states $\rho^o(\epsilon) = (2/\pi D) \sqrt{1 - (\epsilon/D)^2}$, with $t = \frac{D}{2}$, which can be realized in a Bethe lattice and also on a fully connected fully frustrated version of the model [11]. We consider the symmetric case $\mu = 0$. We use an exact diagonalization algorithm (ED) [12] and an extension of the second order perturbative (2OPT) calculation to solve the associated impurity problem [11].

Early work on the optical conductivity in the Hubbard model was carried out by Pruschke *et al.* using quantum Monte Carlo [7], a technique that is restricted to high temperatures. The 2OPT and ED techniques allow us to study the low temperature regime near the Mott transition relevant to the experiments addressed here.

The optical conductivity is defined as $\sigma(\omega) = -\frac{1}{\omega} \text{Im}\langle [j, j] \rangle$. In the limit of $d = \infty$ it can be expressed in terms of the one particle spectrum [7,13],

$$\sigma(\omega) = \frac{1}{\omega} \frac{2e^2 t^2 a^2}{\nu \hbar^2} \int_{-\infty}^{\infty} d\epsilon \rho^o(\epsilon) \int_{-\infty}^{\infty} \frac{d\omega'}{2\pi} A_\epsilon(\omega') A_\epsilon(\omega' + \omega) (n_f(\omega') - n_f(\omega' + \omega)) \quad (3)$$

with $A_\epsilon(\omega) = -2\text{Im}[G_k(\omega)]$, e the electron charge, ν the volume of the unit cell, and a the lattice constant.

At $T = 0$, $\sigma(\omega)$ can be parametrized by $\sigma(\omega) = \frac{\omega_P^{*2}}{4\pi}\delta(\omega) + \sigma_{reg}(\omega)$ where the coefficient in front of the δ -function is the Drude weight and ω_P^* is the renormalized plasma frequency [14]. In the presence of disorder $\delta(\omega)$ is replaced by a lorentzian of width Γ . The expectation value of the kinetic energy $\langle K \rangle$ is related to the conductivity by the sum rule

$$\int_0^\infty \sigma(\omega)d\omega = -\frac{\pi e^2 a^2}{2d\hbar^2\nu}\langle K \rangle = \frac{\omega_P^2}{4\pi} \quad (4)$$

In the limit $d \rightarrow \infty$ the Drude weight is obtained in terms of the quasiparticle weight Z , $\frac{\omega_P^{*2}}{4\pi} = \frac{4\pi t^2 e^2 a^2}{\hbar^2\nu} Z\rho^o(0)$.

The solution of the mean field equations shows that at low temperatures the model has a metal insulator transition (Mott-Hubbard transition) at an intermediate value of the interaction $U_c \approx 3D$ [6–9]. The metallic and insulator solutions at low T are very different and we schematically represent them in Fig. 1. The optical conductivity response, in a first approximation, can be understood from transitions between the states which appear in the the *DOS*. We schematically sketch the optical response in the lower part of Fig. 1.

We will discuss the results for the model in regard of different experimental data on the V_2O_3 system. Vanadium oxide has three t_{2g} orbitals per V atom which are filled with two electrons. Two electrons (one per V) are engaged in a strong cation-cation bond, leaving the remaining two in a twofold degenerate e_g band [15]. LDA calculations give a bandwidth of $\sim 0.5eV$ [16]. The Hubbard model ignores the degeneracy of the band which is crucial in understanding the magnetic structure [15], but captures the interplay of the electron-electron interactions and the kinetic energy. This delicate interplay of itinerancy and localization is responsible for many of the anomalous properties of this compound, and are correctly predicted by this simplified model.

Experimentally one can vary the ratio $\frac{U}{D}$ by introducing V vacancies. The parameters are extracted from the experimental data on $V_{2-y}O_3$ by comparing the measurements with the schematic spectra displayed in Fig. 1, and are summarized in table I. It is not surprising that U and D are different in the metal and the insulator, since the lattice parameter and the screening length change rapidly across the phase boundary.

Our calculations have been performed on the model with nearest neighbor hopping $\frac{t_1}{\sqrt{q}}$ and next to nearest neighbor hopping $\frac{t_2}{q}$ on a Behte lattice. The *n.n.n.* hopping introduces magnetic frustration which is essential if we want to describe V_2O_3 with a one band model. The condition $t_1^2 + t_2^2 = t^2$ keeps the bare density of states ρ^0 invariant. For $t_2/t_1 = 0$ we recover the original hamiltonian, and $t_2/t_1 = 1$ gives the PM solution. The same model on the hypercubic lattice would give very similar results. In Fig. 2 we display the phase diagram for $t_2/t_1 = \sqrt{1/3}$. It has the same topology as the experimental one [10,17,18]. Frustration lowers the T_{Neel} well below the second order T_{MIT} point [9]. Using the parameters of table I, $T_{MIT} \approx 240K$, which is only within less than a factor of 2 from the experimental result. The dotted line indicates a crossover separating a good metal at low T and a semiconductor at higher T . Between these states ρ_{dc} has an anomalous rapid increase with T . The reason for this feature can be traced to the disappearance of the coherent central quasiparticle peak in the *DOS*. We find the behavior of ρ_{dc} to be in good agreement with the experimental results of Mc Whan *et al.* (inset Fig. 2) [18]. Another crossover is indicated by a shaded area, it separates a semiconducting region with a gap Δ comparable with T from a good insulator where $T \ll \Delta$, consequently the crossover temperature increases linearly with U and the crossover width becomes broader with increasing T . This crossover is characterized by a sudden increase in ρ_{dc} as function of U at a fix T (inset Fig. 2). This crossover was experimentally observed in V_2O_3 by Kuwamoto *et al.* [17].

The experimental optical spectrum of the insulator is reproduced in Fig. 3 (dotted lines). It is characterized by an excitation gap at low energies, followed by an incoherent feature that corresponds to charge excitations of mainly Vanadium character [1]. These data are to be compared with the model results of Fig. 4. The size of the gaps Δ (shown for various degrees of magnetic frustration in the inset of Fig. 4), and the overall shape of the spectrum are found to be in good agreement with the experimental results [1]. Another quantity that can be compared to the experiment is the integrated spectral weight $\frac{\omega_P^2}{4\pi}$ which is related to $\langle K \rangle$ by the sum rule (4). Setting the lattice constant $a \approx 3\text{\AA}$ the average $V - V$ distance, we find our results also in good agreement with the experiment (left inset of Fig. 4). Notice that

the dependence of $\langle K \rangle$ and Δ on the degree of magnetic frustration is not very strong, which is consistent with the view that magnetism in this system is not the driving mechanism of the metal insulator transition. Notice also that the experimental points are closer to the intermediate frustration curves than to the unfrustrated ones.

We now discuss the new data in the metallic phase. The experimental data for pure samples that become insulating at $T_c \approx 150K$ were obtained for $T = 170K$ and $T = 300K$, and are presented in Fig. 3 (full lines). Both spectra are made up of broad absorption at higher frequencies and some phonon lines in the far infrared. They appear to be rather featureless, however, upon considering their difference (in which the phonons are approximately eliminated) distinct features are observed. As T is lowered, there is an enhancement of the spectrum at intermediate frequencies of order $0.5eV$; and more notably, a sharp low frequency feature emerges that extends from 0 to $0.15eV$. Moreover, these enhancements result in an anomalous *change* of the total spectral weight $\frac{\omega_P^2}{4\pi}$ with T . We argue below, that these observations can be accounted by the Hubbard model treated in mean field theory.

In Fig. 4 we show the calculated optical spectra obtained from 2OPT for two different values of T . The interaction is set to $U = 2.1D$ that places the system in the correlated metallic state. It is clear that, at least, the qualitative aspect of the physics is already captured. As the temperature is lowered, we observe the enhancement of the incoherent structures at intermediate frequencies of the order $\frac{U}{2}$ to U and the rapid emergence of a feature at the lower end of the spectrum. Setting $D \approx 0.4eV$ we find these results consistent with the experimental data on V_2O_3 . The two emerging features can be interpreted from the qualitative picture that was discussed before which is relevant for low T .

An interesting prediction of the model is the anomalous increase of the integrated spectral weight $\frac{\omega_P^2}{4\pi}$ as T is decreased. This is due to the rather strong T dependence of the kinetic energy $\langle K \rangle \propto \frac{\omega_P^2}{4\pi}$ in the region near the crossover indicated by a dotted line in the phase diagram. This also corresponds with the behavior of the low frequency features in the spectra. From the model calculations we expect an enhancement of the spectral weight as T is decreased. With the chosen parameters this should occur at a scale $T_{coh} \approx 0.05D \approx$

240K which correlates well with the experimental data. T_{coh} has the physical meaning of the temperature below which the Fermi liquid description applies [9], as the quasiparticle resonance emerged in the density of states. We find $\frac{\omega_P^2}{4\pi} \approx 1000 \frac{ev}{\Omega cm}$ which is somewhat lower than the experimental result. This could be due to the contribution from tails of bands at higher energies that are not included in our model, or it may indicate that the bands near the Fermi level are degenerate.

Experiment show that the slope of the linear term in the specific heat γ in the metallic phase is unusually large. For 0.08 *Ti* substitution $\gamma \approx 40 \frac{mJ}{molK^2}$, while for a pressure of 25Kbar in the pure compound $\gamma \approx 30 \frac{mJ}{molK^2}$ and with *V* deficiency in a range of $y = 0.013$ to 0.033 the value is $\gamma \approx 47 \frac{mJ}{molK^2}$ [19]. In our model γ is simply related to the weight in the Drude peak in the optical conductivity and to the quasiparticle residue Z , $\gamma = \frac{1}{ZD} 3 \frac{mJeV}{molK^2}$. The values of $U = 2.1D$ and $D \approx 0.4eV$ extracted from the optical data correspond to a quasiparticle residue $Z \approx 0.3$, and results in $\gamma \approx 25 \frac{mJ}{molK^2}$ which is close to the experimental findings. Thus, it turns out that the mean field theory of the Mott transition explains in a natural and qualitative manner, the experimentally observed optical conductivity spectrum, the anomalously large values of the slope of the specific heat γ , and the dc conductivity in the metallic phase as consequence of the appearance of a single small energy scale, the renormalized Fermi energy ϵ_F^* .

To conclude, we have illustrated how the mean field theory, that becomes exact in the limit of large dimensions, can be used to study the physics of systems where the interactions play a major role. We presented new data on the metallic phase of V_2O_3 revealing an anomalous enhancement of the optical spectral weight as the temperature is lowered in agreement with the surprising prediction of the mean field theory. We also contrasted several experimental results to the solution of the model Hamiltonian to argue that, in the mean field approximation the Hubbard model gives a consistent semiquantitative picture of this strongly correlated electron system. A great challenge is to extend the mean field approach to incorporate more realistic band structure density of states with orbital degeneracies and more complicated unit cells. This extensions will require more efficient tools for solving

larger impurity models, and would allow for a more quantitative description of the physical properties of transition metal oxide systems.

We acknowledge valuable discussions with V. Dobrosavljevic, G. Moeller A. Ruckenstein Q. Si and C.M. Varma. This work was supported by the NSF grant DMR 92-24000

REFERENCES

- * Present Address: LPS, Ecole Normale Supérieure, 24 rue Lhomond, 75231 Paris Cedex, 05 France.
- [1] G. A. Thomas *et al.*, *Phys. Rev. Lett.* **73**, 1529 (1994); G. A. Thomas *et al.*, *Journ. Low Temp. Phys.* **95**, 33 (1994).
- [2] B. Bucher, Z. Schlesinger, P. C. Canfield and Z. Fisk, *Phys. Rev. Lett.* **72**, 522 (1994).
- [3] W. Metzner and D. Vollhardt, *Phys. Rev. Lett.* **62**, 324 (1989).
- [4] A. Georges and G. Kotliar, *Phys. Rev. B* **45**, 6479 (1992).
- [5] A. Georges, G. Kotliar and Q. Si, *Int. J. Mod. Phys. B* **6**, 705 (1992).
- [6] M. Jarrell, *Phys. Rev. Lett.* **69**, 168 (1992); M. J. Rozenberg, X. Y. Zhang and G. Kotliar, *Phys. Rev. Lett.* **69**, 1236 (1992); A. Georges and W. Krauth, *Phys. Rev. Lett.* **69**, 1240 (1992).
- [7] Th. Pruschke, D. L. Cox and M. Jarrell, *Phys. Rev. B* **47**, 3553 (1993).
- [8] A. Georges and W. Krauth, *Phys. Rev. B* **48**, 7167 (1993).
- [9] M. J. Rozenberg, G. Kotliar and X. Y. Zhang, *Phys. Rev. B* **49**, 10181 (1994).
- [10] S. A. Carter, T. F. Rosenbaum, J. M. Honig, and J. Spalek, *Phys. Rev. Lett.* **67**, 3440 (1991).
- [11] X. Y. Zhang, M. J. Rozenberg and G. Kotliar, *Phys. Rev. Lett.* **70**, 1666 (1993).
- [12] M. Caffarel and W. Krauth, *Phys. Rev. Lett.* **72**, 1545 (1994); Q. Si, M. Rozenberg, G. Kotliar and A. Ruckenstein, *Phys. Rev. Lett.* **72**, 2761 (1994); M. J. Rozenberg, G. Moeller, and G. Kotliar, *Mod. Phys. Lett. B* **8**, 535 (1994).
- [13] Anil Khurana, *Phys. Rev. Lett.* **64**, 1990 (1990).
- [14] W. Kohn, *Phys. Rev.* **133**, A171 (1964).

- [15] C. Castellani, C. R. Natoli, and J. Ranninger, *Phys. Rev. B* **18**, 4945 (1978).
- [16] L. F. Mattheiss, *J. Phys., Condens. Matter* **6**, 6477 (1994).
- [17] H. Kuwamoto, J. M. Honig, and J. Appel, *Phys. Rev. B* **22**, 2626 (1980).
- [18] D. Mc Whan *et al.*, *Phys. Rev. B* **7**, 1920 (1973).
- [19] D. Mc Whan *et al.*, *Phys. Rev. Lett.* **27**, 941 (1971); D. Mc Whan *et al.*, *Phys. Rev. B* **7**, 3079 (1973); S. A. Carter *et al.*, *Phys. Rev. B* **48**, 16841 (1993).

FIGURES

FIG. 1. Schematic DOS (1/2 filling) and their corresponding optical spectra for the metallic and insulator solutions. The approximate width of the incoherent peaks in the DOS is $2D$ and that of the central peak in the metal is $ZD \equiv \epsilon_F^*$.

FIG. 2. Approximate phase diagram for the model with $n.n.$ and $n.n.n.$ hopping ($t_2/t_1 = \sqrt{1/3}$). The 1st order PM metal-insulator transition ends at the critical point T_{MIT} (square). The dotted line and the shaded region describe two crossovers as discussed in the text. The full circles indicate the position of the optical spectra. A : insulator ($y = 0$), B : insulator ($y = .013$), C : metal ($y = 0, 170K$), D : metal ($y = 0, 300K$). Note that for comparison with experimental results increasing U/D is associated with decreasing pressure [17,18]. Left inset: $\rho_{dc}(T)$ for $U/D = 2.1, 2.3, 2.5$ (bottom to top). The maxima of $\rho_{dc}(T)$ defines the dotted line. Right inset: $\rho_{dc}(U)$ for $T = 0.06D$ (full) and $T = 0.15D$ (dotted).

FIG. 3. The experimental $\sigma(\omega)$ of metallic V_2O_3 (full lines) at $T = 170K$ (upper) and $T = 300K$ (lower). The inset contains the difference of the two spectra $\Delta\sigma(\omega) = \sigma_{170K}(\omega) - \sigma_{300K}(\omega)$. Diamonds indicate the measured dc conductivity σ_{dc} . Dotted lines indicate $\sigma(\omega)$ of insulating $V_{2-y}O_3$ with $y = .013$ at $10K$ (upper) and $y = 0$ at $70K$ (lower).

FIG. 4. $\sigma(\omega)$ for the metallic solution (full lines) at $U = 2.1D$ and $T = 0.05D$ (upper) and $0.083D$ (lower). A small $\Gamma = 0.3$ and $0.5D$ was included to mimic a finite amount of disorder. Dotted lines indicate the insulating solution results at $U = 4D$ and $T = 0$ from ED (thin-dotted) and 2OPT (bold-dotted). The peaks in ED result from the finite size of the clusters that can be considered. Left inset: $\langle K \rangle$ versus U for the AFM (bold-dotted) and PM insulators (thin), PM metal (bold) and partially frustrated model (thin-dotted). Right inset: Δ versus U for the AFM (dotted), partially frustrated (thin) and PM (bold) insulators. Δ is twice the energy of the lowest pole from the ED Green function. The data are for $N_{sites} \rightarrow \infty$ from clusters of 3, 5 and 7 sites assuming $1/N_{sites}$ scaling behavior. Black squares show the insulator experimental results.

TABLES

Phase	Parameter			
	D [eV]	U [eV]	Δ [eV]	$\omega_P^2/4\pi$ [eV/ Ω cm]
Insulator ($y=0$)	0.33 ± 0.05	1.3 ± 0.05	0.64 ± 0.05	170 ± 20
Insulator ($y=.013$)	0.46 ± 0.05	0.98 ± 0.05	0.08 ± 0.05	800 ± 50
Metal (170K)	0.4 ± 0.1	0.8 ± 0.1	–	1700 ± 300

TABLE I. Experimental parameters for the model.

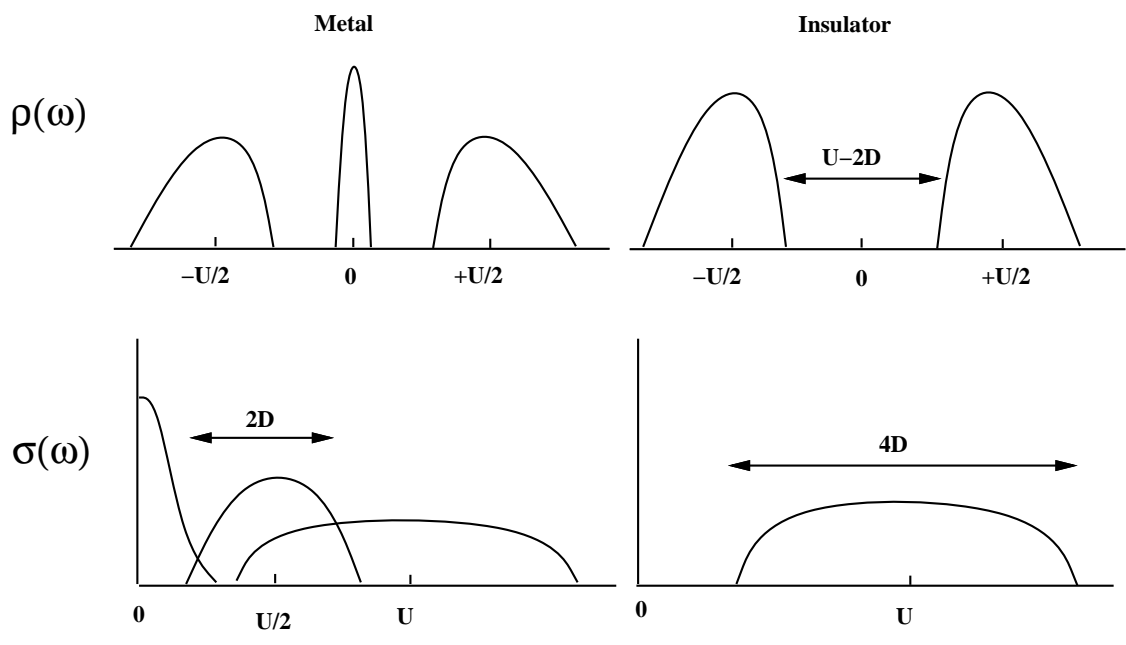


Fig. 1

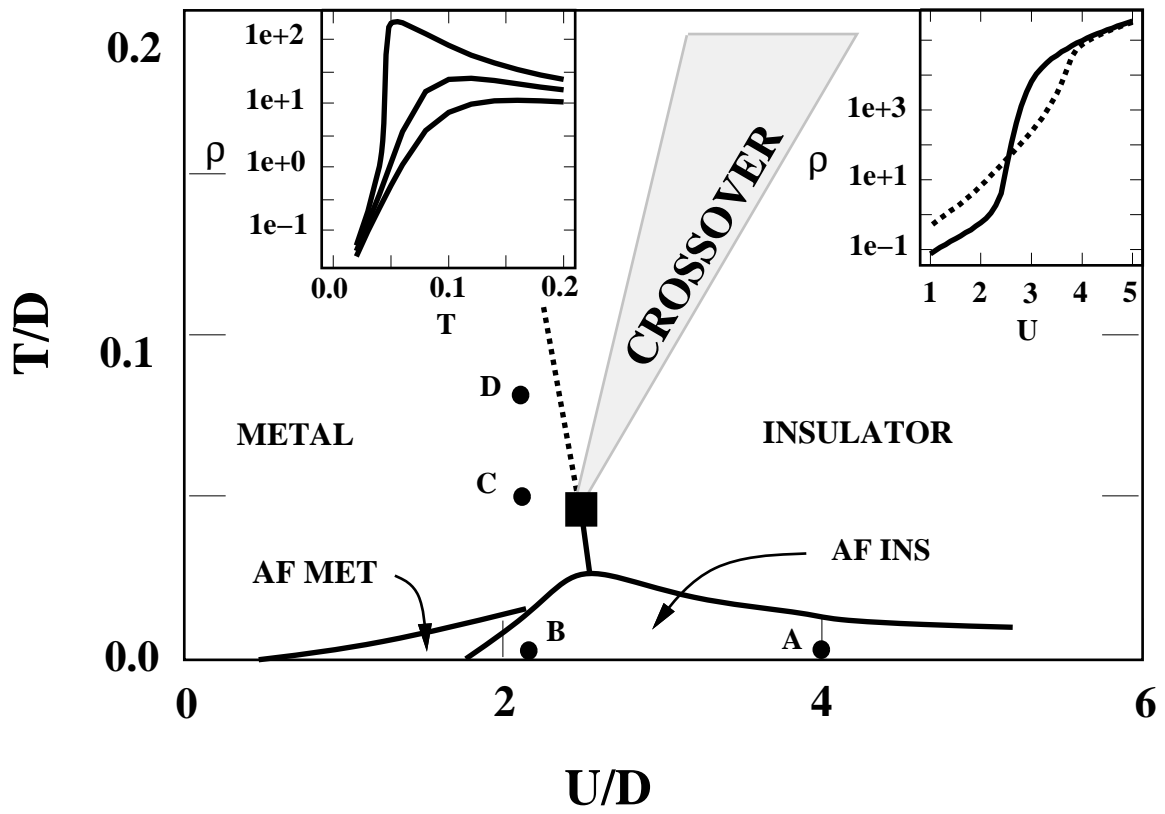


Fig. 2

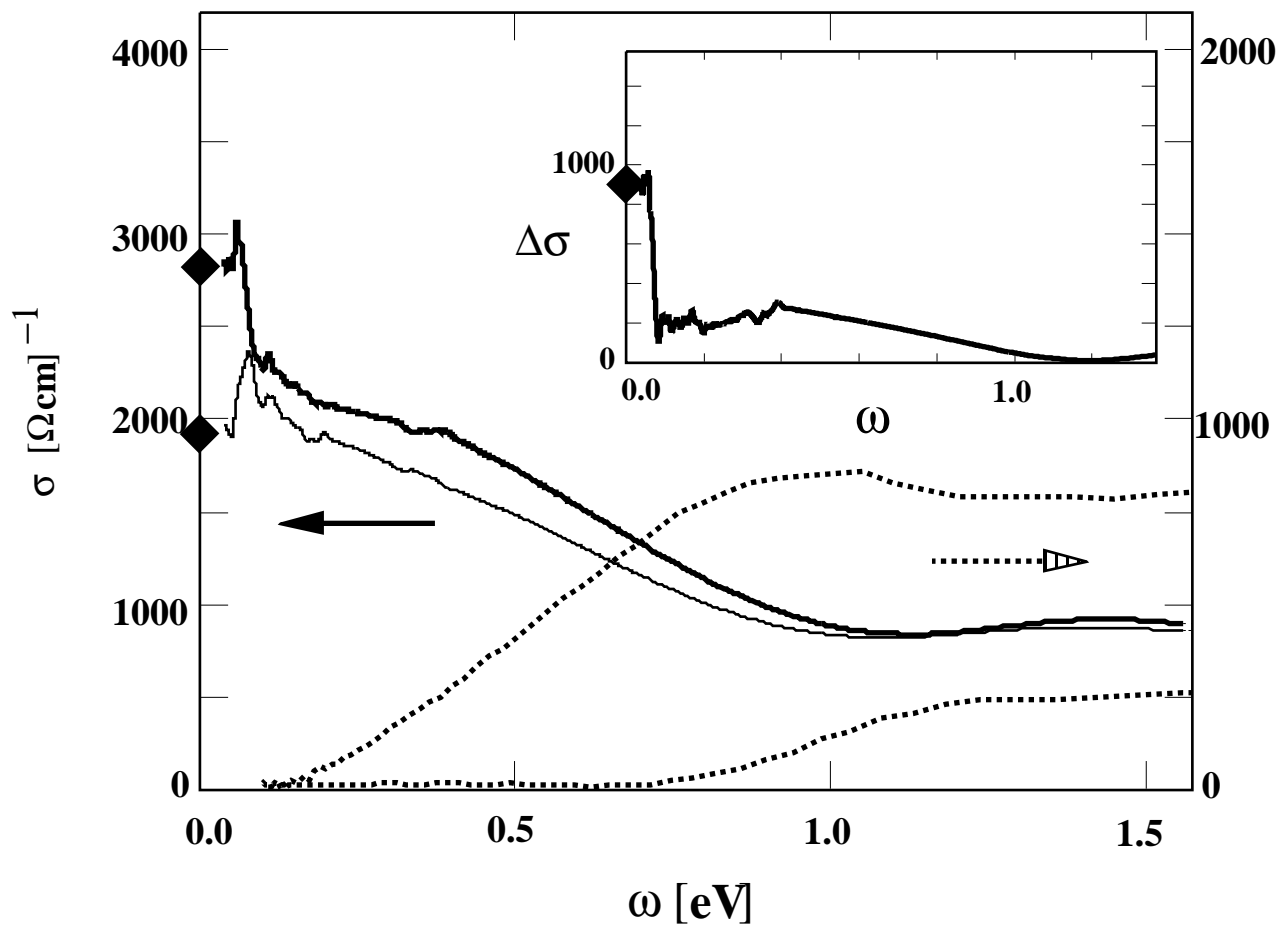


Fig. 3

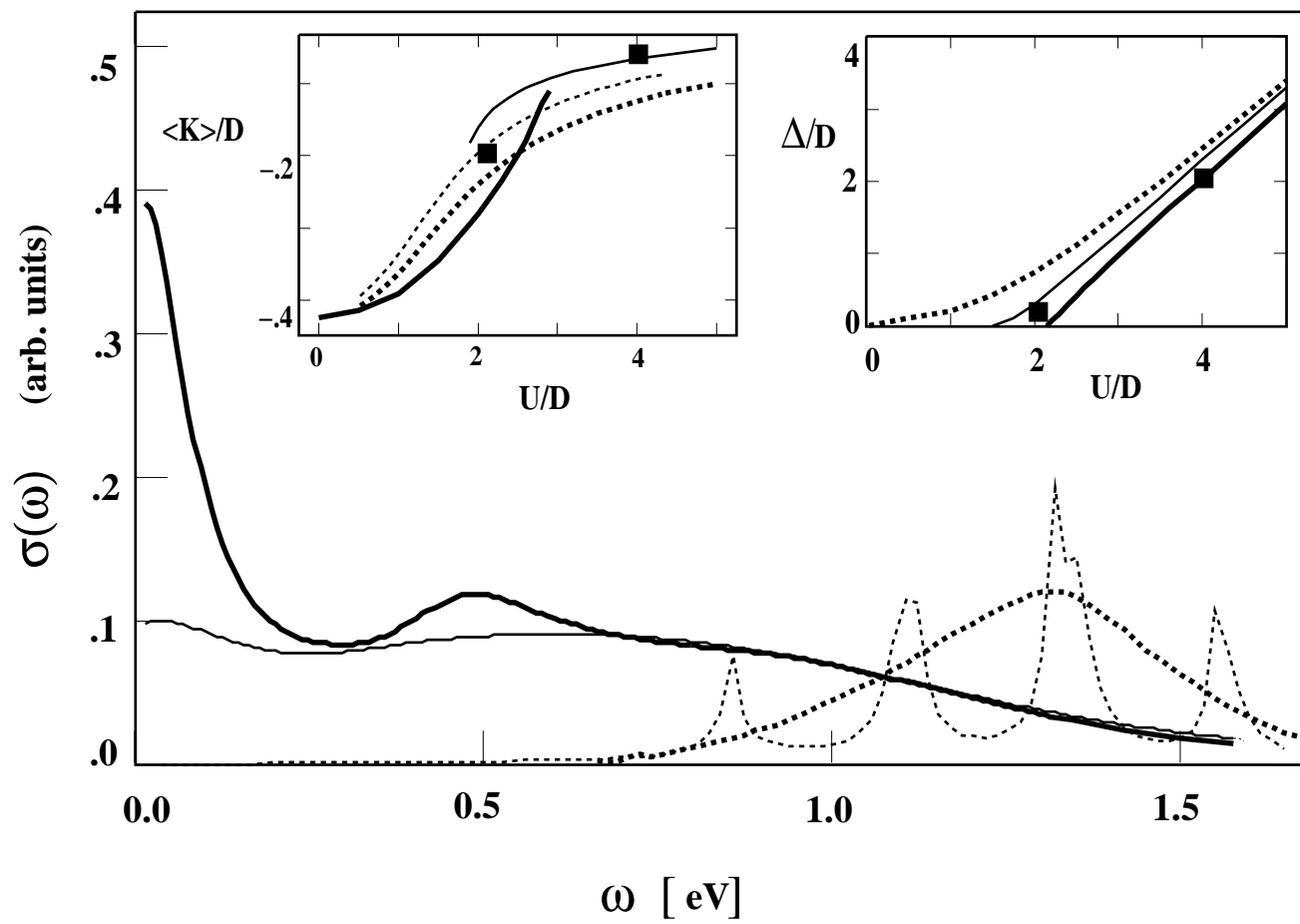


Fig. 4